Wave Motion 98 (2020) 102643

Contents lists available at ScienceDirect

Wave Motion

journal homepage: www.elsevier.com/locate/wamot

Dynamic response of an infinite thin plate loaded with concentrated masses

P.A. Martin [a,1,*], Andrew J. Hull [b,1]

[a] Department of Applied Mathematics and Statistics, Colorado School of Mines, Golden, CO 80401-1887, USA
[b] Undersea Warfare Weapons, Vehicles and Defensive Systems Department, Naval Undersea Warfare Center Division, Newport, RI 02841, USA

ARTICLE INFO

Article history:
Received 2 March 2020
Received in revised form 23 June 2020
Accepted 5 August 2020
Available online 8 August 2020

ABSTRACT

Thin plates with attached concentrated masses are considered. Time-harmonic flexural waves are generated by a force applied over a finite region of the plate. The problem of calculating the resulting plate response reduces to calculating the displacement of the masses, and this is done by solving a finite system of linear algebraic equations in the manner of previous work by Evans and Porter. Numerical results for two masses are presented and compared with finite element computations. Analytical results for N masses arranged around a circle concentric with a circular forcing region are obtained; it is shown that results for a corresponding thin solid ring are recovered as N goes to infinity. Similar results are obtained for a scattering problem, with an incident plane wave.

1. Introduction

Plates that are undergoing dynamic testing frequently have concentrated (or discrete) masses attached to them, either as a component of the structure or as accelerometers to make measurements at specific locations. These masses are sometimes large enough that they influence the response of the structure and thus need to be included in any predictive model. Modal testing of structures has been an ongoing field for many years. Basic modal testing and analysis is discussed by Ewins [1] using measured frequency response functions (FRF). During testing of these structures, accelerometers are used to measure the acceleration at a particular point. Accelerometers are useful instruments because they are relatively inexpensive, accurate and easily affixed to a structure. The major drawback of accelerometers is that they load the structure if they have significant mass and this can cause a distorted measurement.

There are numerous papers that discuss mass loading by accelerometers. Good examples include those by Silva et al. [2], Cakar and Sanliturk [3], Özşahin et al. [4], Bi et al. [5] and Ren et al. [6]. These papers are composed largely of analysis at lower frequencies where the system model is discretized, and then the accelerometer mass is added as a point mass on a discrete element of the structural model.

The problem of a vibrating finite continuous thin plate with concentrated masses also has an extensive literature. The early work is surveyed in Leissa's report [7] and the 1985 paper by Nicholson and Bergman [8] has a good bibliography. For two later studies, see [9] and [10].

* Corresponding author.
E-mail addresses: pamartin@mines.edu (P.A. Martin), andrew.hull@navy.mil (A.J. Hull).
1 Both authors contributed equally to the paper.

https://doi.org/10.1016/j.wavemoti.2020.102643

In this paper, we begin by developing an analytical model of a thin plate carrying N concentrated masses excited by a force applied over a finite region (which we subsequently take to be circular). The plate is taken to be infinite in extent and Kirchhoff–Love theory is used. Thus, for time-harmonic motions, the out-of-plane displacement $w(x, y)$ satisfies the partial differential equation

$$\nabla^4 w - k^4 w = q, \tag{1}$$

where k is the flexural wavenumber and q contains two pieces, one coming from the applied force, and one coming from the concentrated masses; see Eq. (2) below for details. For problems involving circular geometry, such as forcing over a circular region in the presence of a concentric circular solid ring or scattering of a plate wave by a circular inclusion or hole, it is natural to introduce plane polar coordinates leading to separated solutions in terms of Bessel functions [11]. We proceed more directly by working with the two-dimensional Fourier transform of Eq. (1). This leads to an explicit $N \times N$ linear algebraic system of equations for the values of w at the locations of the N concentrated masses. Systems of this kind were obtained by Evans and Porter [12]; the fact that w is finite at the point-mass locations is a consequence of the fourth-order biharmonic operator appearing in Eq. (1). Further applications have been made to infinite periodic arrays of point masses [13–16] and to various configurations of N point masses [14,17–19]. For example, O'Neill et al. [17] investigated how a rigid inclusion may be cloaked by active control of a few point masses in its vicinity.

We give one numerical example in Section 5, where two masses are attached to the plate and a simple forcing is applied over a circular region. The analytical model developed herein is compared to a finite element model to ensure model validation and accuracy of the results obtained.

In Section 6, we consider the problem of N masses arranged evenly around a circle, with forcing applied over a concentric circular region. The symmetry of this problem implies that each mass has the same displacement. We then investigate what happens as $N \to \infty$, and we show that, in the limit, the solution of a related problem for a thin solid ring is obtained. In Section 7, we consider the same problem except we remove the central forcing and replace it with an incident plane wave. This problem is more difficult because one has to calculate the displacement of each mass by solving the $N \times N$ system. The system could be solved numerically (as done by Evans and Porter [12]), but the system matrix is circulant and so it can be inverted analytically. This is done, and then we can investigate the limit as $N \to \infty$. Again, a connection with a related solid ring problem is shown. (The relevant solid ring problems are solved in Appendix B.)

There are some concluding remarks in Section 8.

2. Formulation

Consider an infinite thin plate in the xy-plane. A typical point in the plate has position vector $\boldsymbol{r} = (x, y)$ with respect to a chosen origin. The plate is forced over a region Ω; later, we shall take Ω to be a disc $0 \le r = |\boldsymbol{r}| < a$, and we shall also consider certain scattering problems. In addition, there are N point masses on the plate, located at $\boldsymbol{r} = \boldsymbol{r}_j$, $j = 1, 2, \ldots, N$; the masses are all outside Ω. We assume time-harmonic motions, with a suppressed time dependence of $\mathrm{e}^{-\mathrm{i}\omega t}$.

The basic unknown is the out-of-plane displacement $w(\boldsymbol{r})$. It satisfies

$$\nabla^4 w - k^4 w = f(\boldsymbol{r}) + \sum_{j=1}^{N} \mathcal{M}_j w(\boldsymbol{r}_j)\, \delta(\boldsymbol{r} - \boldsymbol{r}_j). \tag{2}$$

In this equation, the flexural wavenumber $k = \left(\rho h \omega^2 / D\right)^{1/4}$, where the plate has thickness h, density ρ and flexural rigidity $D = Eh^3/(12[1-\nu^2])$; here E is Young's modulus and ν is Poisson's ratio. Also, $\mathcal{M}_j = -m_j\omega^2/D$, where m_j is the mass of the jth point mass on the plate, and δ is the two-dimensional Dirac delta function. The applied forcing is represented by f; when Ω is a disc of radius of a, we take

$$f(\boldsymbol{r}) = f_0 H(a - r) \quad \text{where} \quad f_0 = -\frac{F_0}{\pi a^2 D}, \tag{3}$$

H is the Heaviside unit function and F_0 is the magnitude of the excitation force. Eq. (2) must be supplemented with a radiation condition.

We will solve Eq. (2) in Section 4, but first we solve a simpler problem. This will help explain our methodology in a simpler setting.

3. A simpler problem: Green's function

Consider an infinite plate with point forcing at the origin, so that we have

$$\nabla^4 w - k^4 w = \mathcal{A}\, \delta(\boldsymbol{r}) \tag{4}$$

where $\mathcal{A}$ is a constant (an inverse length, because the two-dimensional $\delta(\boldsymbol{r})$ has dimensions (length)$^{-2}$). We seek a solution representing outgoing waves as $r \to \infty$. In fact, the solution of this problem is well known; we give some references later, below Eq. (12).

To solve Eq. (4), we apply the two-dimensional Fourier transform. (It is traditional to use a Hankel transform but that offers no advantages.) Thus define

$$W(\boldsymbol{s}) = \mathcal{F}\{w\} = \iint w(\boldsymbol{r})\,\mathrm{e}^{-\mathrm{i}\boldsymbol{s}\cdot\boldsymbol{r}}\,\mathrm{d}\boldsymbol{r}, \tag{5}$$

where the integral is over the whole xy-plane. Then we obtain $\Delta(s)\,W(\boldsymbol{s}) = \mathcal{A}$, where

$$\Delta(s) = s^4 - k^4 \quad \text{and} \quad s = |\boldsymbol{s}|.$$

Evidently, $\Delta(s) = 0$ at $s = \pm k$ and at $s = \pm\mathrm{i}k$; we will have to handle these zeros properly, but we shall do that later.

Proceeding formally for now, we have $W = \mathcal{A}/\Delta$ and then, inverting,

$$w(\boldsymbol{r}) = \frac{\mathcal{A}}{(2\pi)^2}\iint \frac{\mathrm{e}^{\mathrm{i}\boldsymbol{s}\cdot\boldsymbol{r}}}{\Delta(s)}\,\mathrm{d}\boldsymbol{s}.$$

Introducing polar coordinates, $\boldsymbol{r} = r(\cos\theta,\ \sin\theta)$ and $\boldsymbol{s} = s(\cos\beta,\ \sin\beta)$, the integration over β is standard; it uses

$$\mathrm{e}^{\mathrm{i}\boldsymbol{s}\cdot\boldsymbol{r}} = \sum_{n=-\infty}^{\infty} \mathrm{i}^n J_n(sr)\,\mathrm{e}^{\mathrm{i}n(\theta-\beta)},$$

where J_n is a Bessel function. Thus we obtain

$$w(\boldsymbol{r}) = \mathcal{A}\,G(r) \quad \text{with} \quad G(r) = \frac{1}{2\pi}\int_0^\infty \frac{J_0(sr)}{s^4 - k^4}\,s\,\mathrm{d}s. \tag{6}$$

In this formula, we must indent the contour below the singularity (a simple pole) at $s = +k$ so that the radiation condition is satisfied. To see this, split the integral into two, using

$$2J_0(sr) = H_0^{(1)}(sr) + H_0^{(2)}(sr), \tag{7}$$

where $H_0^{(1)}$ and $H_0^{(2)}$ are Hankel functions. Thus

$$G(r) = \frac{1}{4\pi}\left(G^{(1)} + G^{(2)}\right) \quad \text{with} \quad G^{(n)}(r) = \int_0^\infty \frac{H_0^{(n)}(sr)}{s^4 - k^4}\,s\,\mathrm{d}s, \quad n = 1, 2. \tag{8}$$

To evaluate $G^{(1)}$, we close the contour using a large quarter-circle in the first quadrant of the complex s-plane and a piece of the positive imaginary axis indented to the right of the pole at $s = +\mathrm{i}k$. This indentation makes a contribution as does the pole at $s = k$ (which is inside the contour). The large quarter-circle does not contribute as its radius increases because of the large-argument behavior of $H_0^{(1)}$. See Appendix A.1 for details. Eventually, we obtain

$$G^{(1)}(r) = \frac{\pi\mathrm{i}}{2k^2}H_0^{(1)}(kr) - \frac{1}{2k^2}K_0(kr) - \frac{2}{\pi\mathrm{i}}\int_0^\infty \frac{K_0(\sigma r)}{\sigma^4 - k^4}\,\sigma\,\mathrm{d}\sigma, \tag{9}$$

where the first term on the right comes from the pole at $s = k$, the second term comes from the pole at $s = \mathrm{i}k$, the last term is a principal-value integral arising from the integral along the positive imaginary axis (from $s = 0$ to $s = +\mathrm{i}\infty$) and K_n is a modified Bessel function.

To evaluate $G^{(2)}$, we close the contour using a large quarter-circle in the fourth quadrant of the s-plane and a piece of the negative imaginary axis indented to the right of the pole at $s = -\mathrm{i}k$. There are no singularities inside the contour. The large quarter-circle does not contribute as its radius increases because of the large-argument behavior of $H_0^{(2)}$. Hence

$$G^{(2)}(r) = -\frac{1}{2k^2}K_0(kr) + \frac{2}{\pi\mathrm{i}}\int_0^\infty \frac{K_0(\sigma r)}{\sigma^4 - k^4}\,\sigma\,\mathrm{d}\sigma. \tag{10}$$

Adding $G^{(1)}$ and $G^{(2)}$, we see that the principal-value integrals cancel, leaving

$$G(r) = \frac{\mathrm{i}}{8k^2}H_0^{(1)}(kr) - \frac{1}{4\pi k^2}K_0(kr). \tag{11}$$

The first term gives outgoing waves (recall that the suppressed time-dependence is $\mathrm{e}^{-\mathrm{i}\omega t}$) whereas the second term decays exponentially with increasing r. Both terms are logarithmically infinite as $r \to 0$ but $G(r)$ is finite at $r = 0$:

$$G(0) = \frac{\mathrm{i}}{8k^2}. \tag{12}$$

This can be shown by letting $r \to 0$ in Eq. (11) or by direct evaluation of the integral defining $G(0)$ (see Appendix A.2). In more detail, starting from Eq. (11), we obtain $G(r) \sim G(0) + (8\pi)^{-1}r^2\log(kr)$ as $r \to 0$, so that $G'(0) = 0$ but $G''(r) \sim (4\pi)^{-1}\log(kr)$ as $r \to 0$.

The formula in Eq. (11) can be found in [20, p. 211], [21, Eq. (7.66)], [11, Eq. (28)] and [12, Eq. (2.3)], for example.

The fact that the outgoing solution of Eq. (4) (which is proportional to $G(r)$, see Eq. (6)) is finite at $r = 0$ (where the point loading is applied) is unusual, and is a consequence of the biharmonic operator in Eq. (4). This fact will be exploited later.

4. Solution of the full problem

Take the two-dimensional Fourier transform of Eq. (2); see Eq. (5). We obtain

$$\Delta(s)\, W(\boldsymbol{s}) = F(\boldsymbol{s}) + \sum_{j=1}^{N} \mathcal{M}_j w(\boldsymbol{r}_j)\, \mathrm{e}^{-\mathrm{i}\boldsymbol{s}\cdot\boldsymbol{r}_j} \tag{13}$$

where $\Delta(s) = s^4 - k^4$, $s = |\boldsymbol{s}|$ and $F = \mathcal{F}\{f\}$. Proceeding formally as in Section 3, we divide by Δ and invert, giving

$$w(\boldsymbol{r}) = w_f(\boldsymbol{r}) + \sum_{j=1}^{N} w_j \mathcal{M}_j\, G(|\boldsymbol{r} - \boldsymbol{r}_j|), \tag{14}$$

where $w_j = w(\boldsymbol{r}_j)$, G is given by Eq. (11) and

$$w_f(\boldsymbol{r}) = \frac{1}{(2\pi)^2} \iint \frac{F(\boldsymbol{s})}{\Delta(s)}\, \mathrm{e}^{\mathrm{i}\boldsymbol{s}\cdot\boldsymbol{r}}\, \mathrm{d}\boldsymbol{s}. \tag{15}$$

Eq. (14) gives $w(\boldsymbol{r})$ everywhere once we have computed $w_f(\boldsymbol{r})$ and the N complex numbers w_i, $i = 1, 2, \ldots, N$. To find these numbers, we simply collocate Eq. (14) at $\boldsymbol{r} = \boldsymbol{r}_i$, giving

$$w_i - \sum_{j=1}^{N} w_j \mathcal{M}_j\, G(|\boldsymbol{r}_i - \boldsymbol{r}_j|) = w_f(\boldsymbol{r}_i), \quad i = 1, 2, \ldots, N, \tag{16}$$

recalling that $G(0)$ is finite, see Eq. (12). Thus we have an $N \times N$ linear algebraic system for the displacements of the point masses, Eq. (16). Once solved, $w(\boldsymbol{r})$ is given by Eq. (14).

The method used here is essentially that developed by Evans and Porter [12]. See especially [12, §3] where results for scattering of a plane wave by N point masses equally spaced around a circle are given; we shall return to this problem in Section 7.

Evidently, $w = w_f$ in the absence of the point masses, so that w_f itself must represent outgoing waves. When f is axisymmetric and given by Eq. (3), $w_f(r)$ can be evaluated explicitly (Appendix A.3); see Eq. (A.6) when $r > a$ and Eq. (A.7) when $0 \le r < a$.

The far field

When $kr \gg 1$, we can approximate the exact solution, Eq. (14). As the modified Bessel function $K_0(kr)$ in Eq. (11) decays exponentially, it can be discarded, and we retain the large-argument approximation for $H_0^{(1)}(kr)$ [22, 10.2.5]. We can do the same with w_f when f is given by Eq. (3), see Eq. (A.6). Hence

$$w(\boldsymbol{r}) = w(r,\theta) \sim \sqrt{\frac{2}{\pi}}\, \mathrm{e}^{-\mathrm{i}\pi/4} \frac{\mathrm{e}^{\,\mathrm{i}kr}}{\sqrt{kr}} \left\{F_f + F_N(\theta)\right\} \quad \text{as } kr \to \infty, \tag{17}$$

where $\hat{\boldsymbol{r}} = \boldsymbol{r}/r = (\cos\theta,\ \sin\theta)$ gives the direction of observation. The quantity $F_f + F_N$ is the *far-field pattern*. The first part, F_f, is due to the forcing itself; from Eq. (A.6),

$$F_f = \frac{\mathrm{i}\pi f_0 a}{4k^3} J_1(ka). \tag{18}$$

Of more interest is $F_N(\theta)$, coming from the N point masses. Using $|\boldsymbol{r} - \boldsymbol{r}_j| \sim r - \hat{\boldsymbol{r}} \cdot \boldsymbol{r}_j$ as $r \to \infty$, we obtain

$$F_N(\theta) = \frac{\mathrm{i}}{8k^2} \sum_{j=1}^{N} w_j \mathcal{M}_j \exp\left(-\mathrm{i}k\hat{\boldsymbol{r}} \cdot \boldsymbol{r}_j\right). \tag{19}$$

5. Application: a numerical example with two masses

A numerical example problem is now developed and compared to finite element analysis (FEA) for model validation. The system parameters are as follows: Young's modulus $E = 2.00 \times 10^8(1 - 0.2\mathrm{i})$ Pa, Poisson's ratio $\nu = 0.45$, thickness $h = 0.002$ m, density $\rho = 1100\,\mathrm{kg\,m^{-3}}$, frequency $\omega/2\pi = 100$ Hz, applied load radius $a = 0.0254$ m, magnitude of applied force $F_0 = 1$ N. (We have included some simple structural damping by choosing E to be complex; this makes the FEA computations easier because the computational domain has to be truncated.) These give a flexural rigidity of $D = 0.1672 - 0.0334\mathrm{i}$ N m and a flexural wavenumber of $k = 47.45 + 2.34\mathrm{i}\,\mathrm{m}^{-1}$.

For this validation problem, there are two attached masses. Their masses and locations are given by m_j and $\boldsymbol{r}_j = r_j(\cos\theta_j, \sin\theta_j)$, respectively, with $j = 1, 2$. We take $m_1 = 0.01$ kg, $r_1 = 0.2032$ m, $\theta_1 = \pi/2$, $m_2 = 0.02$ kg, $r_2 = 0.3048$ m and $\theta_2 = \pi/4$.

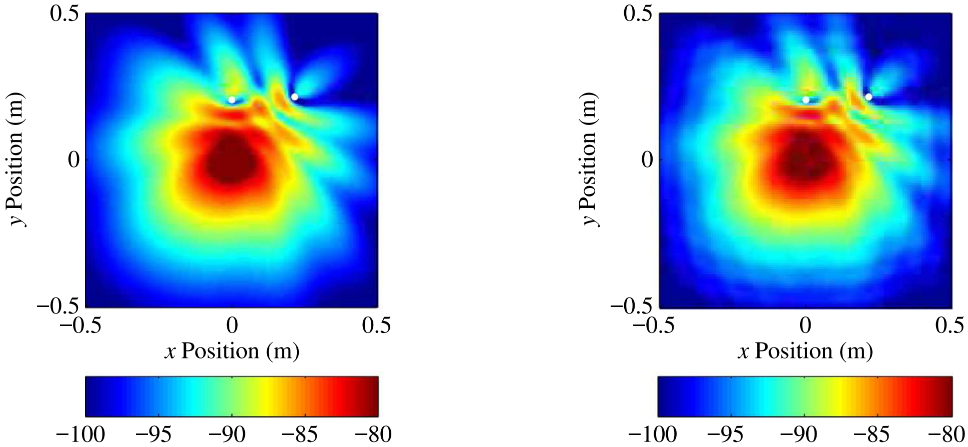

Fig. 1. Normal displacement in the xy-plane for the analytical model (left) and the finite element model (right) when there is central forcing and two attached masses (indicated by the small white circular markers). The scale is decibels referenced to meters.

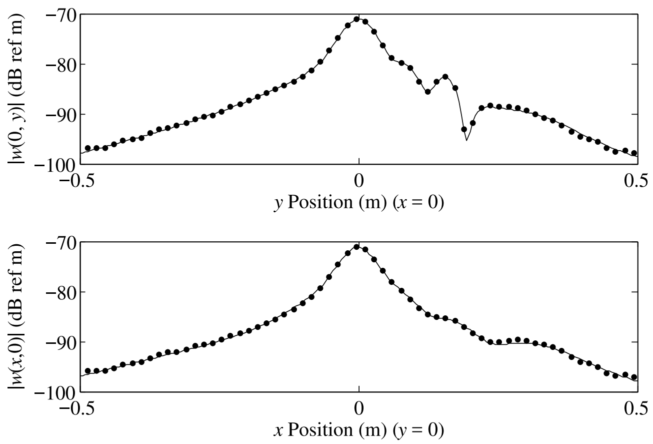

Fig. 2. Normal displacement for the analytical model (solid line) and the finite element model (circular markers) when there is central forcing and two attached masses. The scale is decibels referenced to meters.

The problem is formulated and the analytical results are compared to the FEA results graphically. Fig. 1 gives two-dimensional plots of the magnitude of the normal displacement of the plate in the xy-plane, $|w(x, y)|$, using the analytical model developed in Section 4 (left) and the finite element model (right), displayed using a decibel scale referenced to meters. The locations of the masses are depicted with two single white circular markers. There is broad based agreement between the analytical model and the finite element model, indicating that the models are producing very similar responses. Fig. 2 shows a more detailed comparison along the x-axis and along the y-axis (which passes through the second attached mass).

6. Application: a circular ring of point masses

Suppose we have N point masses, all of mass m, equally spaced around the circle $r = b$, with $b > a$. Let $h = 2\pi/N$ be the angular spacing between adjacent masses; they are located at $\boldsymbol{r} = \boldsymbol{r}_j = b(\cos\theta_j,\ \sin\theta_j)$ where $\theta_j = jh$ and $j = 1, 2, \ldots, N$. (Note that $\boldsymbol{r}_0 = \boldsymbol{r}_N$.)

We assume that the forcing is provided by Eq. (3) implying that the masses have the same displacement; thus $w_j = w_0$ and $\mathcal{M}_j = \mathcal{M}$ for $j = 1, 2, \ldots, N$, where $\mathcal{M} = -m\omega^2/D$.

From Eq. (16), w_0 is given by

$$w_0 = \frac{w_f(b)}{1 - \Omega_N(\boldsymbol{r}_0)} \quad \text{with} \quad \Omega_N(\boldsymbol{r}_0) = \mathcal{M} \sum_{j=1}^{N} G(|\boldsymbol{r}_j - \boldsymbol{r}_0|), \tag{20}$$

where $w_f(r)$ is given by Eq. (A.6) and $|\boldsymbol{r}_j - \boldsymbol{r}_0| = b\sqrt{2-2\cos\theta_j} = 2b\,|\sin(jh/2)|$. Then Eq. (14) gives

$$w(r) = w_f(r) + \frac{w_f(b)\,\Omega_N(\boldsymbol{r})}{1-\Omega_N(\boldsymbol{r}_0)}.$$

The component of the far-field pattern associated with the N masses, $F_N(\theta)$ (see Eq. (17)), is given by

$$F_N(\theta) = \frac{\mathrm{i}}{8k^2}\,w_0 E_N(\theta) = \frac{\mathrm{i}}{8k^2}\,w_f(b)\,\frac{E_N(\theta)}{1-\Omega_N(\boldsymbol{r}_0)}$$

(see Eq. (19)), where

$$E_N(\theta) = \mathcal{M}\sum_{j=1}^{N}\exp\{-\mathrm{i}kb\cos(jh-\theta)\}.$$

Let us suppose now that N is large. Intuitively, we expect that F_N should approach that for a solid thin ring of radius b. Suppose the solid ring has mass M_r, and then choose the mass of each point mass according to $Nm = M_\mathrm{r}$. Equivalently, we have $N\mathcal{M} = \mathcal{M}_\mathrm{r} = -M_\mathrm{r}\omega^2/D$ as $\mathcal{M} = -m\omega^2/D$. Hence, as $h = 2\pi/N$,

$$\begin{aligned} E_N(\theta) &= \frac{\mathcal{M}_\mathrm{r}}{2\pi}\,h\sum_{j=1}^{N}\mathrm{e}^{-\mathrm{i}kb\cos(jh-\theta)} \\ &\sim \frac{\mathcal{M}_\mathrm{r}}{2\pi}\int_0^{2\pi}\mathrm{e}^{-\mathrm{i}kb\cos(\vartheta-\theta)}\mathrm{d}\vartheta = \mathcal{M}_\mathrm{r}J_0(kb) \end{aligned}$$

as $N\to\infty$. This follows because the sum can be seen as a way of approximating the integral by the trapezoidal rule. Moreover, as the integrand is smooth and 2π-periodic, the error is exponentially small as a function of N [23].

Let us now examine $\Omega_N(\boldsymbol{r}_0)$. From Eq. (11) and Eq. $(20)_2$, we have

$$\begin{aligned} \Omega_N(\boldsymbol{r}_0) &= \frac{\mathcal{M}_\mathrm{r}}{2\pi}\,h\sum_{j=1}^{N}G(2kb\,|\sin(jh/2)|) \\ &\sim \frac{\mathcal{M}_\mathrm{r}}{2\pi}\int_0^{2\pi}G(2kb\,|\sin(\vartheta/2)|)\,\mathrm{d}\vartheta = \mathcal{M}_\mathrm{r}\,\mathcal{L}_0 \end{aligned} \tag{21}$$

as $N\to\infty$, where, from Eq. (A.3),

$$\mathcal{L}_n = \frac{\mathrm{i}}{8k^2}H_n^{(1)}(kb)J_n(kb) - \frac{1}{4\pi k^2}K_n(kb)I_n(kb) = \mathcal{L}_{-n}. \tag{22}$$

However, although the integrand in Eq. (21) is 2π-periodic with one continuous derivative, its second derivative is logarithmically infinite at $\vartheta = 0$ and $\vartheta = 2\pi$ (see the discussion below Eq. (12)). Consequently, the limit Eq. (21) is achieved rather slowly, $O(N^{-2})$ as $N\to\infty$ [24, p. 30, Example 2], [25, Theorem 1.19].

Comparison with the solution of the solid-ring problem (see Appendix B.1) shows that we do obtain the corresponding far-field pattern as $N\to\infty$, but, as already noted, this limit is reached rather slowly as the number of masses increases.

7. Application: scattering by a ring of point masses

We consider the same geometry as in Section 6, with a ring of N identical, equally-spaced point masses. However, we suppose that the forcing is provided by an incident plane wave instead of the central forcing used in Section 6. This has the effect that the motion of each mass has to be calculated because we no longer have an axisymmetric problem.

Before specializing to a ring, let us start with the problem of scattering by N point masses, with arbitrary locations and masses. Let w denote the total displacement field. It satisfies Eq. (2) with $f\equiv 0$. The incident wave w_in satisfies $\nabla^4 w_\mathrm{in} - k^4 w_\mathrm{in} = 0$ everywhere so that the scattered field $w_\mathrm{sc} = w - w_\mathrm{in}$ satisfies

$$\nabla^4 w_\mathrm{sc} - k^4 w_\mathrm{sc} = \sum_{j=1}^{N} w_j\mathcal{M}_j\,\delta(\boldsymbol{r}-\boldsymbol{r}_j), \tag{23}$$

together with a radiation condition. Here, $w_j = w(\boldsymbol{r}_j)$, as before. Solving Eq. (23), we obtain (see Eq. (14) with $w_f\equiv 0$)

$$w_\mathrm{sc}(\boldsymbol{r}) = \sum_{j=1}^{N} w_j\mathcal{M}_j\,G(|\boldsymbol{r}-\boldsymbol{r}_j|). \tag{24}$$

To find the complex numbers w_j, we evaluate at each point-mass location. As $w_{\rm sc}(\boldsymbol{r}_j) = w_j - w_{\rm in}(\boldsymbol{r}_j)$, we obtain an $N \times N$ system,

$$w_i - \sum_{j=1}^{N} w_j \mathcal{M}_j\, G(|\boldsymbol{r}_i - \boldsymbol{r}_j|) = w_{\rm in}(\boldsymbol{r}_i), \quad i = 1, 2, \ldots, N. \tag{25}$$

Evidently, this system has the same structure as Eq. (16). It is [12, Eq. (3.3)].

Let us return to scattering by a ring of point masses. The incident wave is

$$w_{\rm in}(\boldsymbol{r}) = \mathcal{W}\, {\rm e}^{{\rm i}kx}$$

where $\mathcal{W}$ is a constant (a length). As $\mathcal{M}_j = \mathcal{M}$ and $|\boldsymbol{r}_i - \boldsymbol{r}_j| = 2b|\sin\{(i-j)h/2\}|$ with $h = 2\pi/N$, the system Eq. (25) reduces to

$$\sum_{j=1}^{N} C_{i-j} w_j = g_i, \quad i = 1, 2, \ldots, N, \tag{26}$$

where $g_j = \mathcal{W} \exp({\rm i}kb\cos jh)$,

$$C_0 = 1 - \mathcal{M}G(0), \quad C_j = -\mathcal{M}\, G(2b|\sin(jh/2)|), \quad j \neq 0 \bmod N$$

and C_j is N-periodic: $C_{j+mN} = C_j$, $m = \pm 1, \pm 2, \ldots$.

Movchan et al. [19] have considered the homogeneous version of Eq. (26), and found non-trivial solutions for certain complex values of k.

Evans and Porter [12, §3] gave some numerical solutions of Eq. (26) for $N = 4$ and $N = 8$. However, it is notable that Eq. (26) can be solved explicitly, for any N, because the system matrix in Eq. (26) is a circulant matrix; see [26] and [27] for details and related applications. Thus introduce discrete Fourier transforms (DFTs),

$$w_n = \frac{1}{N} \sum_{j=1}^{N} \widetilde{w}_j\, \varpi^{-nj} \quad \text{and} \quad \widetilde{w}_n = \sum_{j=1}^{N} w_j\, \varpi^{nj} \tag{27}$$

where $\varpi = {\rm e}^{2\pi{\rm i}/N} = {\rm e}^{{\rm i}h}$. Then the DFT of the solution to Eq. (26) is given by $\widetilde{w}_j = \widetilde{g}_j/\widetilde{C}_j$ with

$$\widetilde{g}_n = \sum_{j=1}^{N} g_j\, \varpi^{nj} \quad \text{and} \quad \widetilde{C}_n = \sum_{j=1}^{N} C_j\, \varpi^{nj}.$$

Having determined w_n, the displacement anywhere in the plate is given by Eq. (24),

$$w(\boldsymbol{r}) = w_{\rm in}(\boldsymbol{r}) + \mathcal{M} \sum_{j=1}^{N} w_j\, G(|\boldsymbol{r} - \boldsymbol{r}_j|). \tag{28}$$

In particular, at the center of the ring, $w(\mathbf{0}) = \mathcal{W} + \mathcal{M}\, G(b)\, \widetilde{w}_0$, and the far-field pattern is

$$F_N(\theta) = \frac{{\rm i}\mathcal{M}}{8k^2} \sum_{j=1}^{N} w_j\, {\rm e}^{-{\rm i}kb\cos(jh-\theta)} = \frac{{\rm i}\mathcal{M}}{8k^2} \sum_{n=-\infty}^{\infty} \widetilde{w}_n (-{\rm i})^n J_n(kb)\, {\rm e}^{-{\rm i}n\theta}. \tag{29}$$

Suppose now that N is large. Proceeding as in Section 6, with $\mathcal{M} = \mathcal{M}_{\rm r}/N$,

$$\frac{1}{N}\widetilde{g}_n = \frac{\mathcal{W}}{2\pi} h \sum_{j=1}^{N} {\rm e}^{{\rm i}kb\cos(jh)} {\rm e}^{{\rm i}njh} \sim \frac{\mathcal{W}}{2\pi} \int_0^{2\pi} {\rm e}^{{\rm i}kb\cos\theta} {\rm e}^{{\rm i}n\theta}\, {\rm d}\theta = \mathcal{W}\, {\rm i}^n J_n(kb)$$

as $N \to \infty$, with exponentially fast convergence.

Similarly, but with a much slower rate of convergence, we have

$$\begin{aligned} \widetilde{C}_n &= 1 - \frac{\mathcal{M}_{\rm r}}{2\pi} h \sum_{j=1}^{N} G(2b|\sin(jh/2)|)\, {\rm e}^{{\rm i}njh} \\ &\sim 1 - \frac{\mathcal{M}_{\rm r}}{2\pi} \int_0^{2\pi} G(2b|\sin(\vartheta/2)|)\, {\rm e}^{{\rm i}n\vartheta}\, {\rm d}\vartheta = 1 - \mathcal{M}_{\rm r}\, \mathcal{L}_n \end{aligned}$$

as $N \to \infty$, using Eq. (A.3). Then, using $\mathcal{M} = \mathcal{M}_{\rm r}/N$ and $\widetilde{w}_n = \widetilde{g}_n/\widetilde{C}_n$, Eq. (29) gives the estimate

$$F_N(\theta) \sim \frac{{\rm i}\mathcal{M}_{\rm r}}{8k^2} \mathcal{W} \sum_{n=-\infty}^{\infty} \frac{J_n^2(kb)}{1 - \mathcal{M}_{\rm r}\mathcal{L}_n} {\rm e}^{-{\rm i}n\theta} \quad \text{as } N \to \infty.$$

This limiting result agrees with the corresponding result for a solid ring, Eq. (B.8).

8. Discussion

The method described in this paper provides an efficient way to compute the effect of any number of attached point masses on wave propagation in an infinite thin plate. It could be extended to problems where the masses have rotary inertia; this leads to a modified form of Eq. (2) in which there are additional terms involving the gradient of w evaluated at the mass locations [28, Eq. (3)].

Future work will consider thick plates with attached discrete masses. This will allow analysis for a much higher frequency range and it will provide an ability to model greater plate thicknesses. It will, however, produce a model of significantly greater complexity.

Declaration of competing interest

The authors declare that they have no known competing financial interests or personal relationships that could have appeared to influence the work reported in this paper.

Acknowledgments

The authors wish to thank Anthony J. Paolero, Naval Undersea Warfare Center, for his help in developing the finite element model. Funding for Andrew J. Hull was partially provided by the Naval Undersea Warfare Center, USA's In-house Independent Laboratory Research (ILIR) Program. Paul Martin thanks his colleague, Bernard Bialecki, for pointing out the result in the Russian book [24] used below Eq. (22).

Appendix A. Evaluation of some integrals

A.1. Evaluation of $G(r)$

We give a few more details of the computations outlined in Section 3. After splitting G as Eq. (8), we start with $G^{(1)}(r)$, $r > 0$. Close the contour with a large quarter-circle in the first quadrant of the complex s-plane. The large-argument behavior of $H_0^{(1)}$ [22, 10.2.5] ensures that the quarter-circle does not contribute as its radius grows. The pole at $s = k$ makes a residue contribution of

$$2\pi\mathrm{i}\frac{1}{4k^2}H_0^{(1)}(kr).$$

Thus

$$G^{(1)}(r) + \int_{C_1} \frac{H_0^{(1)}(sr)}{s^4 - k^4}\, s\,\mathrm{d}s = \frac{\pi\mathrm{i}}{2k^2}H_0^{(1)}(kr), \tag{A.1}$$

where the contour C_1 comes down the positive imaginary axis (from $s = +\mathrm{i}\infty$ to $s = 0$) indented to the right of the pole at $s = \mathrm{i}k$. The indentation contributes

$$-\pi\mathrm{i}\frac{\mathrm{i}k}{4(\mathrm{i}k)^3}H_0^{(1)}(\mathrm{i}kr) = \frac{1}{2k^2}K_0(kr),$$

using [22, 10.27.8]. The straight parts of C_1 give a principal-value integral; if we put $s = \mathrm{i}\sigma$ on that piece of the contour, we see that

$$\begin{aligned}\int_{C_1} &= \frac{1}{2k^2}K_0(kr) + \int_\infty^0 \frac{H_0^{(1)}(\mathrm{i}\sigma r)}{\sigma^4 - k^4}\,\mathrm{i}\sigma\,(\mathrm{i}\,\mathrm{d}\sigma)\\ &= \frac{1}{2k^2}K_0(kr) + \frac{2}{\pi\mathrm{i}}\int_0^\infty \frac{K_0(\sigma r)}{\sigma^4 - k^4}\,\sigma\,\mathrm{d}\sigma.\end{aligned}$$

Substitution in Eq. (A.1) leads to Eq. (9).

For $G^{(2)}(r)$, we close the contour with a large quarter-circle in the fourth quadrant of the s-plane. The large-argument behavior of $H_0^{(2)}$ [22, 10.2.6] ensures that the quarter-circle does not contribute as its radius grows. There are no poles inside the contour. Hence

$$G^{(2)}(r) + \int_{C_2} \frac{H_0^{(2)}(sr)}{s^4 - k^4}\, s\,\mathrm{d}s = 0 \tag{A.2}$$

where the contour C_2 goes up the negative imaginary axis (from $s = -\mathrm{i}\infty$ to $s = 0$) indented to the right of the pole at $s = -\mathrm{i}k$. The indentation contributes

$$\pi\mathrm{i}\frac{-\mathrm{i}k}{4(-\mathrm{i}k)^3}H_0^{(2)}(-\mathrm{i}kr) = \frac{1}{2k^2}K_0(kr).$$

The straight parts of C_2 give a principal-value integral; if we put $s = -\mathrm{i}\sigma$ on that piece of the contour, we see that

$$\int_{C_2} = \frac{1}{2k^2}K_0(kr) + \int_\infty^0 \frac{H_0^{(2)}(-\mathrm{i}\sigma r)}{\sigma^4 - k^4}(-\mathrm{i}\sigma)(-\mathrm{i}\,\mathrm{d}\sigma)$$
$$= \frac{1}{2k^2}K_0(kr) - \frac{2}{\pi\mathrm{i}}\int_0^\infty \frac{K_0(\sigma r)}{\sigma^4 - k^4}\,\sigma\,\mathrm{d}\sigma.$$

Substitution in Eq. (A.2) leads to Eq. (10).

A certain integral of G is needed in Sections 6 and 7. It is

$$\frac{1}{2\pi}\int_0^{2\pi} G(2kb\,|\sin(\vartheta/2)|)\,\mathrm{e}^{\mathrm{i}n\vartheta}\,\mathrm{d}\vartheta = \frac{2}{\pi}\int_0^{\pi/2} G(2kb\sin\vartheta)\cos 2n\vartheta\,\mathrm{d}\vartheta$$
$$= \frac{\mathrm{i}}{4\pi k^2}\int_0^{\pi/2} H_0^{(1)}(2kb\sin\vartheta)\cos 2n\vartheta\,\mathrm{d}\vartheta - \frac{1}{2\pi^2k^2}\int_0^{\pi/2} K_0(2kb\sin\vartheta)\cos 2n\vartheta\,\mathrm{d}\vartheta$$
$$= \frac{\mathrm{i}}{8k^2}H_n^{(1)}(kb)J_n(kb) - \frac{1}{4\pi k^2}K_n(kb)I_n(kb) = \mathcal{L}_n, \tag{A.3}$$

say. The integrals were evaluated using formulas (6), (7) and (13) in [29, §6.681]. See also [19, §3.3].

A.2. Direct evaluation of $G(0)$

The evaluation of $G(0)$ is elementary. We give this evaluation because it can be used to check the value of $G(r)$ as $r \to 0$. We use partial fractions, paying attention to potential divergences. As $J_0(0) = 1$, Eq. (6) gives

$$G(0) = \frac{1}{2\pi}\int_0^\infty \frac{s\,\mathrm{d}s}{s^4 - k^4} = \frac{1}{4\pi k^2}\int_0^\infty \left(\frac{s}{s^2 - k^2} - \frac{s}{s^2 + k^2}\right)\mathrm{d}s.$$

Then, for any $X > k$,

$$\int_0^X \frac{s\,\mathrm{d}s}{s^2 + k^2} = \frac{1}{2}\left[\log(s^2 + k^2)\right]_0^X = \frac{1}{2}\log(X^2 + k^2) - \log k,$$
$$\frac{1}{2k^2}\int_0^X \frac{s\,\mathrm{d}s}{s^2 - k^2} = \frac{1}{4k^2}\int_0^X \left(\frac{1}{s-k} + \frac{1}{s+k}\right)\mathrm{d}s,$$
$$\int_0^X \frac{\mathrm{d}s}{s+k} = \log(X + k) - \log k.$$

Finally, consider the remaining integral, $\int_0^X (s-k)^{-1}\,\mathrm{d}s$. The contour is indented below the pole at $s = k$. This indentation contributes $\pi\mathrm{i}$. The rest of the integral leads to a principal-value integral,

$$\lim_{\varepsilon\to 0}\left(-\int_0^{k-\varepsilon}\frac{\mathrm{d}s}{k-s} + \int_{k+\varepsilon}^X \frac{\mathrm{d}s}{s-k}\right) = \lim_{\varepsilon\to 0}\left([\log(k-s)]_0^{k-\varepsilon} + [\log(s-k)]_{k+\varepsilon}^X\right)$$
$$= \log(X-k) - \log k.$$

Assembling all the pieces, we have

$$G(0) = \frac{1}{8\pi k^2}\lim_{X\to\infty}\left(\pi\mathrm{i} + \log\frac{X^2 - k^2}{X^2 + k^2}\right) = \frac{\mathrm{i}}{8k^2}.$$

A.3. Evaluation of w_f

The function w_f is defined by Eq. (15) in terms of $F = \mathcal{F}\{f\}$. We shall evaluate w_f when the forcing is given by Eq. (3). In that case, we have

$$F(\boldsymbol{s}) = \int_\Omega f(\boldsymbol{r})\,\mathrm{e}^{-\mathrm{i}\boldsymbol{s}\cdot\boldsymbol{r}}\,\mathrm{d}\boldsymbol{r} = f_0\int_0^a\int_0^{2\pi} \mathrm{e}^{-\mathrm{i}sr\cos(\theta-\beta)}\,r\,\mathrm{d}\theta\,\mathrm{d}r$$
$$= 2\pi f_0\int_0^a J_0(sr)\,r\,\mathrm{d}r = 2\pi f_0\frac{a}{s}J_1(sa). \tag{A.4}$$

Then substitution in Eq. (15) gives

$$w_f(\boldsymbol{r}) = \frac{f_0 a}{2\pi}\iint \frac{J_1(sa)}{\Delta(s)}\mathrm{e}^{\mathrm{i}sr\cos(\theta-\beta)}\,\frac{\mathrm{d}\boldsymbol{s}}{s}$$
$$= f_0 a\int_0^\infty \frac{J_1(sa)J_0(sr)}{s^4 - k^4}\,\mathrm{d}s. \tag{A.5}$$

In this formula, the contour is indented below the singularity at $s = k$ so that the radiation condition is satisfied. Also, we shall write $w_f(r)$ for $w_f(\boldsymbol{r})$.

Suppose first that $r > a$. We proceed as in Appendix A.1. Using Eq. (7), we write

$$w_f(r) = \frac{f_0 a}{2}\left(w_f^{(1)} + w_f^{(2)}\right)$$

where

$$w_f^{(n)}(r) = \int_0^\infty \frac{J_1(sa)}{s^4 - k^4}\, H_0^{(n)}(sr)\,\mathrm{d}s, \quad n = 1, 2.$$

Using the same notation as in Appendix A.1, we obtain

$$w_f^{(1)}(r) + \int_{C_1} \frac{J_1(sa)}{s^4 - k^4}\, H_0^{(1)}(sr)\,\mathrm{d}s = 2\pi\mathrm{i}\frac{J_1(ka)}{4k^3}\, H_0^{(1)}(kr),$$

$$w_f^{(2)}(r) + \int_{C_2} \frac{J_1(sa)}{s^4 - k^4}\, H_0^{(2)}(sr)\,\mathrm{d}s = 0.$$

For C_1, the indentation to the right of $s = \mathrm{i}k$ contributes

$$-\pi\mathrm{i}\frac{J_1(\mathrm{i}ka)}{4(\mathrm{i}k)^3}\, H_0^{(1)}(\mathrm{i}kr) = \frac{1}{2k^3}\, I_1(ka)\, K_0(kr)$$

whereas for C_2 the indentation to the right of $s = -\mathrm{i}k$ contributes

$$\pi\mathrm{i}\frac{J_1(-\mathrm{i}ka)}{4(-\mathrm{i}k)^3}\, H_0^{(2)}(-\mathrm{i}kr) = \frac{1}{2k^3}\, I_1(ka)\, K_0(kr).$$

The principal-value part of the integral along C_1 is

$$\int_\infty^0 \frac{J_1(\mathrm{i}\sigma a)}{\sigma^4 - k^4}\, H_0^{(1)}(\mathrm{i}\sigma r)\,(\mathrm{i}\,\mathrm{d}\sigma) = \frac{2}{\pi\mathrm{i}}\int_0^\infty \frac{I_1(\sigma a)}{\sigma^4 - k^4}\, K_0(\sigma r)\,\mathrm{d}\sigma$$

whereas the principal-value part of the integral along C_2 is

$$\int_\infty^0 \frac{J_1(-\mathrm{i}\sigma a)}{\sigma^4 - k^4}\, H_0^{(2)}(-\mathrm{i}\sigma r)\,(-\mathrm{i}\,\mathrm{d}\sigma) = -\frac{2}{\pi\mathrm{i}}\int_0^\infty \frac{I_1(\sigma a)}{\sigma^4 - k^4}\, K_0(\sigma r)\,\mathrm{d}\sigma.$$

Adding $w_f^{(1)}$ and $w_f^{(2)}$, the principal-value integrals cancel, and we are left with

$$w_f(r) = \frac{f_0 a}{2k^3}\left\{\frac{\pi\mathrm{i}}{2} J_1(ka)\, H_0^{(1)}(kr) - I_1(ka)\, K_0(kr)\right\}, \quad r > a. \tag{A.6}$$

Suppose next that $r < a$ (so that we are evaluating w_f at points in Ω). In order to have proper decay at infinity, we split $J_1(sa)$ in Eq. (A.5), using $2J_1(sa) = H_1^{(1)}(sa) + H_1^{(2)}(sa)$, but this introduces singularities at $s = 0$ because $H_1^{(1)}(z) \sim -H_1^{(2)}(z) \sim 2/(\pi\mathrm{i}z)$ as $z \to 0$.

We integrate $H_1^{(1)}(sa)J_0(sr)(s^4 - k^4)^{-1}$ around a closed contour $\mathcal{C}_1$ comprising a piece from $s = \varepsilon$ to $s = R$ passing below the pole at $s = k$; a large quarter-circle from $s = R$ to $s = \mathrm{i}R$; a piece from $s = \mathrm{i}R$ to $s = \mathrm{i}\varepsilon$, indented to the right of the pole at $s = \mathrm{i}k$; and a small quarter-circle from $s = \mathrm{i}\varepsilon$ to $s = \varepsilon$. Similarly, we integrate $H_1^{(2)}(sa)J_0(sr)(s^4 - k^4)^{-1}$ around a closed contour $\mathcal{C}_2$ comprising a piece from $s = \varepsilon$ to $s = R$ passing below the pole at $s = k$; a large quarter-circle from $s = R$ to $s = -\mathrm{i}R$; a piece from $s = -\mathrm{i}R$ to $s = -\mathrm{i}\varepsilon$, indented to the right of the pole at $s = -\mathrm{i}k$; and a small quarter-circle from $s = -\mathrm{i}\varepsilon$ to $s = \varepsilon$. The pole at $s = k$ is inside $\mathcal{C}_1$ but outside $\mathcal{C}_2$. Proceeding as before, the large quarter-circles do not contribute as $R \to \infty$ and, when the two integrals are added, it is found that the two-principal-value integrals from integrating along the imaginary axis cancel. The indentations at $s = \pm\mathrm{i}k$ contribute equally, as do the two small quarter-circles as $\varepsilon \to 0$. We obtain

$$w_f(r) = \frac{f_0 a}{2k^3}\left\{\frac{\pi\mathrm{i}}{2}\, H_1^{(1)}(ka)J_0(kr) + K_1(ka)\, I_0(kr) - \frac{2}{ka}\right\}, \quad r < a. \tag{A.7}$$

Eqs. (A.6) and (A.7) agree with formulas obtained by Klanner and Ellermann [30, Eq. (3.25)] using a different method. Moreover, using Wronskians, we can check that $w_f(r)$ is continuous at $r = a$.

Appendix B. Ring problems

We consider two problems involving thin-plate waves in the presence of a thin circular ring of mass M_r and radius b. We have not found solutions of these problems in the literature; there are a few papers on free vibrations of circular plates with a concentric circular support [31–35]. For such geometries, separated solutions in plane polar coordinates can be used [11].

B.1. An axisymmetric problem

Consider the axisymmetric problem with waves forced by Eq. (3). The governing equation is

$$\nabla^4 w - k^4 w = f(\boldsymbol{r}) + \mathcal{M}_\mathrm{r}\,(2\pi b)^{-1} w(b)\,\delta(r-b), \tag{B.1}$$

where $\mathcal{M}_\mathrm{r} = -M_\mathrm{r}\omega^2/D$. The Fourier transform of Eq. (B.1) is

$$\Delta(s)\,W(\boldsymbol{s}) = F(\boldsymbol{s}) + \mathcal{M}_\mathrm{r} J_0(sb)\,w(b).$$

Dividing by Δ and inverting gives

$$w(r) = w_f(r) + \mathcal{M}_\mathrm{r}\,w(b)\,\mathcal{J}_0(r,b), \tag{B.2}$$

where

$$\mathcal{J}_n(r,b) = \frac{1}{2\pi}\int_0^\infty \frac{J_n(sr)J_n(sb)}{s^4-k^4}\,s\,\mathrm{d}s = \mathcal{J}_n(b,r) = \mathcal{J}_{-n}(r,b). \tag{B.3}$$

The method used to evaluate $G(r)$ can be used to show that

$$\mathcal{J}_n(r,b) = \frac{\mathrm{i}}{8k^2}\,H_n^{(1)}(kr)J_n(kb) - \frac{1}{4\pi k^2}\,K_n(kr)\,I_n(kb), \quad r > b. \tag{B.4}$$

As a check, $\mathcal{J}_0(r,b)$ reduces to $G(r)$ when $b=0$; see Eq. $(6)_2$ and Eq. (11).

From Eq. (B.2), $(1-\mathcal{M}_\mathrm{r}\,\mathcal{L}_0)\,w(b) = w_f(b)$, where we have noted that $\mathcal{J}_n(b,b) = \mathcal{L}_n$; compare Eq. (A.3) with Eq. (B.4). Hence

$$w(r) = w_f(r) + \frac{\mathcal{M}_\mathrm{r}\,w_f(b)\,\mathcal{J}_0(r,b)}{1-\mathcal{M}_\mathrm{r}\,\mathcal{L}_0}.$$

The corresponding far-field pattern (see Eq. (17)) is $F_f + F_\mathrm{r}$, where F_f is given by Eq. (18) and

$$F_\mathrm{r} = \frac{\mathrm{i}}{8k^2}\,w_f(b)\,\frac{\mathcal{M}_\mathrm{r} J_0(kb)}{1-\mathcal{M}_\mathrm{r}\,\mathcal{L}_0}. \tag{B.5}$$

B.2. A scattering problem

Let us replace Eq. (B.1) by

$$\nabla^4 w_\mathrm{sc} - k^4 w_\mathrm{sc} = \mathcal{M}_\mathrm{r}\,(2\pi b)^{-1} w(b,\theta)\,\delta(r-b), \tag{B.6}$$

with $w_\mathrm{sc} = w - w_\mathrm{in}$ giving outgoing waves. The Fourier transform of this equation is

$$\Delta(s)\,W_\mathrm{sc}(\boldsymbol{s}) = \mathcal{M}_\mathrm{r}\sum_{n=-\infty}^{\infty}(-\mathrm{i})^n J_n(sb)\,\mathrm{e}^{\mathrm{i}n\beta}\,\hat{w}_n,$$

where we have used the Fourier expansion $w(b,\theta) = \sum_n \hat{w}_n\,\mathrm{e}^{\mathrm{i}n\theta}$, which means

$$\hat{w}_n = \frac{1}{2\pi}\int_{-\pi}^{\pi} w(b,\theta)\,\mathrm{e}^{-\mathrm{i}n\theta}\,\mathrm{d}\theta.$$

Inverting $W_\mathrm{sc} = \mathcal{F}\{w_\mathrm{sc}\}$ gives

$$w_\mathrm{sc}(r,\theta) = \mathcal{M}_\mathrm{r}\sum_{n=-\infty}^{\infty}\hat{w}_n\,\mathcal{J}_n(r,b)\,\mathrm{e}^{\mathrm{i}n\theta}, \tag{B.7}$$

with $\mathcal{J}_n$ defined by Eq. (B.3). To find $\hat{w}_n$, we use

$$w_\mathrm{sc}(b,\theta) = w(b,\theta) - w_\mathrm{in}(b,\theta) = \sum_{n=-\infty}^{\infty}\left\{\hat{w}_n - \mathcal{W}\,\mathrm{i}^n J_n(kb)\right\}\mathrm{e}^{\mathrm{i}n\theta}$$

and $\mathcal{J}_n(b,b) = \mathcal{L}_n$, whence

$$\hat{w}_n(1-\mathcal{M}_\mathrm{r}\mathcal{L}_n) = \mathcal{W}\,\mathrm{i}^n J_n(kb).$$

The far field can be obtained from Eq. (B.7), using Eq. (B.4) and [22, 10.2.5]. The corresponding far-field pattern is

$$\begin{aligned} F(\theta) &= \frac{\mathrm{i}\mathcal{M}_\mathrm{r}}{8k^2}\sum_{n=-\infty}^{\infty}(-\mathrm{i})^n\hat{w}_n J_n(kb)\,\mathrm{e}^{\mathrm{i}n\theta} \\ &= \frac{\mathrm{i}\mathcal{M}_\mathrm{r}}{8k^2}\,\mathcal{W}\sum_{n=-\infty}^{\infty}\frac{J_n^2(kb)}{1-\mathcal{M}_\mathrm{r}\,\mathcal{L}_n}\,\mathrm{e}^{\mathrm{i}n\theta}. \end{aligned} \tag{B.8}$$

References

[1] D.J. Ewins, Modal Testing: Theory, Practice and Application, second ed., Baldock, Research Studies Press Ltd., 2000.
[2] J.M.M. Silva, N.M.M. Maia, A.M.R. Ribeiro, Cancellation of mass-loading effects of transducers and evaluation of unmeasured frequency response functions, J. Sound Vib. 236 (2000) 761–779.
[3] O. Cakar, K.Y. Sanliturk, Elimination of transducer mass loading effects from frequency response functions, Mech. Syst. Signal Process. 19 (2005) 87–104.
[4] O. Özşahin, H.N. Özgüven, E. Budak, Analysis and compensation of mass loading effect of accelerometers on tool point FRF measurements for chatter stability predictions, Int. J. Mach Tools Manuf. 50 (2010) 585–589.
[5] S. Bi, J. Ren, W. Wang, G. Zong, Elimination of transducer mass loading effects in shaker modal testing, Mech. Syst. Signal Process. 38 (2013) 265–275.
[6] J. Ren, J. Wang, S. Bi, Correction of transducers mass effects from the measured FRFs in hammer impact testing, Shock Vib. 2017 (2017) 6857326, 10.
[7] A.W. Leissa, Vibration of Plates, NASA Report SP-160, Washington, D.C, 1969.
[8] J.W. Nicholson, L.A. Bergman, Vibration of thick plates carrying concentrated masses, J. Sound Vib. 103 (1985) 357–369.
[9] D.V. Bambill, S. La Malfa, C.A. Rossit, P.A.A. Laura, Analytical and experimental investigation on transverse vibrations of solid, circular and annular plates carrying a concentrated mass at an arbitrary position with marine applications, Ocean Eng. 31 (2004) 127–138.
[10] D. Li, J. Zhang, Mobility matrix of a thin circular plate carrying concentrated masses based on transverse vibration solution, Shock Vib. 2014 (2014) 284367, 15.
[11] A.N. Norris, C. Vemula, Scattering of flexural waves on thin plates, J. Sound Vib. 181 (1995) 115–125.
[12] D.V. Evans, R. Porter, Penetration of flexural waves through a periodically constrained thin elastic plate in vacuo and floating on water, J. Engrg. Math. 58 (2007) 317–337.
[13] S.G. Haslinger, N.V. Movchan, A.B. Movchan, R.C. McPhedran, Transmission, trapping and filtering of waves in periodically constrained elastic plates, Proc. R. Soc. Lond. Ser. A Math. Phys. Eng. Sci. 468 (2012) 76–93.
[14] C.G. Poulton, A.B. Movchan, N.V. Movchan, R.C. McPhedran, Analytic theory of defects in periodically structured elastic plates, Proc. R. Soc. Lond. Ser. A Math. Phys. Eng. Sci. 468 (2012) 1196–1216.
[15] R.C. McPhedran, A.B. Movchan, N.V. Movchan, M. Brun, M.J.A. Smith, Parabolic trapped modes and steered Dirac cones in platonic crystals, Proc. R. Soc. Lond. Ser. A Math. Phys. Eng. Sci. 471 (2015) 20140746, 22.
[16] S.G. Haslinger, N.V. Movchan, A.B. Movchan, I.S. Jones, R.V. Craster, Controlling flexural waves in semi-infinite platonic crystals with resonator-type scatterers, Q. J. Mech. Appl. Math. 70 (2017) 215–247.
[17] J. O'Neill, Ö. Selsil, R.C. McPhedran, A.B. Movchan, N.V. Movchan, Active cloaking of inclusions for flexural waves in thin elastic plates, Q. J. Mech. Appl. Math. 68 (2015) 263–288.
[18] G.J. Chaplain, M.P. Makwana, R.V. Craster, Rayleigh–Bloch topological edge and interface waves for structured elastic plates, Wave Motion 86 (2019) 162–174.
[19] A.B. Movchan, R.C. McPhedran, G. Carta, R.V. Craster, Platonic localisation: one ring to bind them, Arch. Appl. Mech. 89 (2019) 521–533.
[20] M. Kitahara, Boundary Integral Equation Methods in Eigenvalue Problems of Elastodynamics and Thin Plates, Elsevier, Amsterdam, 1985.
[21] M.C. Junger, D. Feit, Sound, Structures, and their Interaction, second ed., Acoustical Society of America, New York, 1993.
[22] Digital library of mathematical functions, 2019, dlmf.nist.gov.
[23] L.N. Trefethen, J.A.C. Weideman, The exponentially convergent trapezoidal rule, SIAM Rev. 56 (2014) 385–458.
[24] A.A. Samarskii, R.D. Lazarov, V.L. Makarov, Difference Schemes for Differential Equations with Generalized Solutions (in Russian), Vysshaya Shkola, Moscow, 1987.
[25] D. Cruz-Uribe, C.J. Neugebauer, Sharp error bounds for the trapezoidal rule and Simpson's rule, J. Inequal Pure Appl. Math. 3 (2002) 22, paper no. 49.
[26] R. Vescovo, Electromagnetic scattering from cylindrical arrays of infinitely long thin wires, Electron. Lett. 31 (1995) 1646–1647.
[27] P.A. Martin, On acoustic and electric Faraday cages, Proc. R. Soc. Lond. Ser. A Math. Phys. Eng. Sci. 470 (2014) 20140344, 14.
[28] A.H. Shah, S.K. Datta, Normal vibrations of a rectangular plate with attached masses, J. Appl. Mech. 36 (1969) 130–132.
[29] I.S. Gradshteyn, I.M. Ryzhik, Table of Integrals, Series, and Products, fourth ed., Academic Press, New York, 1980.
[30] M. Klanner, K. Ellermann, Solutions of vibration problems for thin infinite plates subjected to harmonic loads, J. Theor. Appl. Mech. 55 (2017) 949–961.
[31] R.Y. Bodine, The fundamental frequency of a thin, flat, circular plate simply supported along a circle of arbitrary radius, J. Appl. Mech. 26 (1959) 666–668.
[32] R.Y. Bodine, Vibrations of a circular plate supported by a concentric ring of arbitrary radius, J. Acoust. Soc. Am. 41 (1967) 1551.
[33] C.L. Kirk, A.W. Leissa, Vibration characteristics of a circular plate with a concentric reinforcing ring, J. Sound Vib. 5 (1967) 278–284.
[34] P.A.A. Laura, R.H. Gutiérrez, S.A. Vera, D.A. Vega, Transverse vibrations of a circular plate with a free edge and a concentric circular support, J. Sound Vib. 223 (1999) 842–845.
[35] C.Y. Wang, On the fundamental frequency of a circular plate supported on a ring, J. Sound Vib. 243 (2001) 945–946.